ceramics

MDPI

Article

Properties of a Pressureless Sintered 2Y-TZP Material Combining High Strength and Toughness

Frank Kern * and Bettina Osswald

Institute for Manufacturing Technologies of Ceramic Components and Composites, Faculty 7: Engineering Design, Production Engineering and Automotive Engineering, University of Stuttgart, Allmandring 7b, 70569 Stuttgart, Germany

* Correspondence: frank.kern@ifkb.uni-stuttgart.de

Abstract: Yttria stabilized zirconia materials are frequently used in mechanical engineering and biomedical applications. Demanding loading conditions require materials combining a high level of strength and fracture toughness. A ready-to-press alumina doped 2 mol% yttria-stabilized zirconia powder was shaped by axial pressing and sintering in air at 1250–1500 °C for 2 h. At 1350 °C the best combination of strength (1450 MPa) and toughness (7.8 MPa$\sqrt{m}$) was achieved. Materials sintered in the middle of the chosen temperature range combine full density, high transformability and small grain size. Toughness measurements by direct crack length measurements delivered unrealistically high fracture toughness values.

Keywords: zirconia; high toughness; microstructure; phase composition

check for updates

Citation: Kern, F.; Osswald, B. Properties of a Pressureless Sintered 2Y-TZP Material Combining High Strength and Toughness. *Ceramics* **2024**, *7*, 893–905. https://doi.org/10.3390/ceramics7030058

Academic Editor: Malika Saadaoui

Received: 22 May 2024
Revised: 24 June 2024
Accepted: 26 June 2024
Published: 28 June 2024

Copyright: © 2024 by the authors. Licensee MDPI, Basel, Switzerland. This article is an open access article distributed under the terms and conditions of the Creative Commons Attribution (CC BY) license (https://creativecommons.org/licenses/by/4.0/).

1. Introduction

Partially stabilized zirconia materials are structural ceramics which combine high strength and fracture toughness by exploiting the effect of transformation toughening (TT) [1]. TT describes a reinforcement mechanism based on the martensitic transformation of metastable tetragonal phase to stable monoclinic phase associated with volume expansion and shear. If a crack in partially stabilized zirconia is exposed to tensile stress, a transformation zone forms at the crack tip. As the crack expands, the transformation zone in the wake of the crack exerts compressive stress which leads to reduction of the stress intensity at the crack tip. The shear component can be accommodated by twin-like orientation of the transformed monoclinic domains [2,3]. In order to obtain a metastable tetragonal phase after sintering, zirconia has to be stabilized by the addition of oxides containing aliovalent or isovalent cations which stabilize the tetragonal phase by expanding the lattice, by introduction of oxygen vacancies or both [4,5]. Today, yttria is probably the technologically most important stabilizer oxide. As yttria is trivalent, yttria addition introduces oxygen vacancies to retain charge neutrality. Moreover, as Y^{3+} is an oversized dopant (larger than Zr^{4+}), additional stabilization by lattice expansion is obtained. Yttria forms tetragonal and cubic solid solutions with zirconia [6]. The yttria content in yttria stabilized tetragonal zirconia polycrystals (Y-TZP) is typically adjusted at 3 mol% Y_2O_3 (3Y-TZP) [7]. At a typical sintering temperature of ~1400 °C, 3Y-TZP is a composition within the t + c field, a miscibility gap. At this temperature, this gap ranges from 2.5 to 6.5 mol% Y_2O_3 [6]. Hence, 3Y-TZP sintered at this temperature should, by rule of the lever, decompose to ~20% cubic and ~80% tetragonal phase. However, as the powders are typically produced by co-precipitation, the initial distribution of yttria in zirconia is homogeneous at atomic level. Phase segregation is therefore inhibited and requires high sintering temperatures [8]. The tetragonal phase in 3Y-TZP sintered at moderate temperatures is, therefore, super-saturated and not very transformable. This leads to materials with high strength (>1000 MPa) but very moderate toughness (4–6 MPa$\sqrt{m}$) [9]. In order to improve the toughness of Y-TZP produced from co-precipitated powder two pathways are possible. The first is to sinter

TZP at temperatures >>1500 °C for long dwell time to trigger the phase segregation and increase the grain size of the tetragonal grains to make the material more transformable [10]. The second is to reduce the stabilizer content to a level of 2.5 mol% to obtain an entirely tetragonal material. Further reduction of the stabilizer content below 2.5 mol% leads to a more transformable tetragonal phase [11]. Both procedures face some difficulties. The first route leads to very coarse-grained materials with reduced strength. At the same time these materials become very prone to degrade by low temperature degradation (LTD) in the presence of humidity [12]. In case of the second route, it has to be considered that the critical grain size beyond which the material will transform spontaneously during cooling from sintering temperature is reduced with declining stabilizer content [13]. This requires very fine and sinterable starting powders to obtain fully dense and fine rain ceramics at moderate sintering temperatures. Moreover, we may expect that entirely tetragonal compositions with a stabilizer content <2.5 mol% will show less stabilizer segregation to the grain boundary which prevents grain growth by solute drag [8]. The concept has been known for decades and is well described in the literature [14]. The difficulties described above have for a long time prevented implementation of understabilized Y-TZP, as it was considered too dangerous to use for fear of spontaneous transformation and LTD. Recently different powder producers offer fine understabilized Y-TZPs (with 1.5–2 mol% Y_2O_3) and there are a few new studies. Innovnano's 2Y-TZP, which was produced by detonation synthesis, delivered an impressive combination of strength and toughness but has disappeared from the market [15]. Tosoh's ZGAIA 1.5Y-TZP promised extreme toughness in combination with attractive strength [16]. Recent studies by Imariouane showed that indentation toughness values were exaggerated; still, a fracture toughness of 9 MPa$\sqrt{m}$ combined with a strength of 1000 MPa is respectable [17].

The material is, however, tricky to sinter and requires high cooling rates to retain the metastable tetragonal phase [18]. In the present study, a new alumina doped 2Y-TZP issued by Treibacher Industries in Austria was tested and compared to literature values shown in Table 1. Literature values appear controversial. On the one hand, this is due to different strength and toughness measurement protocols. Ref. [15] allows a comparison of three different strength measurement protocols, with 4PB being the strictest. Concerning the toughness measurement, the DCM method seems to deliver systematically higher values than conservative methods. Kern shows that in the compositional range between 1.5Y and 2Y-TZP, strength and toughness show adverse trends [19]. Further deviations are presumably caused by powder properties, shaping technology and sintering protocols.

Table 1. Strength and toughness data for Y-TZP with 1.5–2 mol% Y_2O_3 stabilizer.

Composition Mol% Y_2O_3	Strength [1] [MPa]	Toughness [2] [MPa$\sqrt{m}$]	References
1.5	1088, 3PB	14.5, DCM	[11]
		4.7, SCF	
1.5	2600, P3B	13.8, DCM	[20]
1.5	1438, P3B	4.8, SEVNB	[21]
1.5	1270, 3PB	22, DCM	[16]
1.5	995, 4PB	8.5, SEVNB	[17]
	1320, 3B3B		
2	994 3PB	6.4, SEVNB	[22]
2	1560, 4PB	9.6, ISB	[15]
	2088, P3B		
	1670, 3B3B		
2	n.d.	5.9, DCM	[23]

Table 1. *Cont.*

Composition Mol% Y_2O_3	Strength [1] [MPa]	Toughness [2] [MPa$\sqrt{m}$]	References
2 (3Y + 0Y)	1270, 3PB	10.3, DCM	[19]
1.5 (3Y + 0Y)	630, 3PB	14.5, DCM	
1.75 (3Y + 0Y)	680, 3PB	10.3, DCM	
2 (3Y + 0Y)	1050, 3PB	8, DCM	
2	1250, BA	7.7, DCM	[24]

[1] Abbreviations for strength measurement: 3PB = 3pt bending, 4PB = 4pt bending, P3B = piston on three balls, 3B3B = three balls on three balls, BA = biaxial; [2] Abbreviations for toughness measurement: DCM = direct crack length measurement (indentation toughness), SCF = surface crack in flexure, SEVNB = single edge V-notched beam, ISB = indentation strength in flexure.

2. Materials and Methods

The starting material used in this study is a zirconia powder stabilized with 2 mol% of yttria and alloyed with 0.4 wt-% of alumina. The powder was delivered as a ready to press (RTP) granulate by the manufacturer (Auertec® 2Y-40A-B, Treibacher, Althofen, Austria, S_{BET} = 11.15 m^2/g). The loss on ignition (correlates to binder content) was specified as 4.3 wt-%. The granules had an average diameter of 45 µm. The powder was cold-pressed in a rectangular steel die of 35 × 35 mm^2 diameter (Graveurbetrieb Leonhardt, Hochdorf, Germany) at 125 MPa pressure in a manually operated press (Paul Weber, Remshalden, Germany). An amount of 9 g of powder were weighed per plate resulting in a sintered plate of approx. 2 mm thickness. The plates were subsequently debindered in air (1 °C/min to 600 °C, 3 h dwell, Linn, Eschenfelden, Germany) and sintered in air in a dental furnace (MIHM-Vogt HT speed, Stutensee, Germany) at 2 °C/min to 1200 °C and 1 °C/min to final temperature (1250–1500 °C in 50 °C increments). Cooling was carried out at 12 °C/min to room temperature.

The plates (4 plates per sintering temperature) were then lapped on both sides with 15 µm diamond suspension and polished on one side with 15 µm, 6 µm, 3 µm and 1 µm diamond suspension to obtain a mirror-like finish using an automatic machine (Struers Rotopol, Copenhagen, Denmark). The plates were cut into bars with 4 mm width (Struers Accutom, Copenhagen, Denmark) with a diamond wheel. The as-cut sides were lapped with 15 µm suspension to remove cutting-induced defects. Finally, the edges were beveled manually using a 40 µm diamond disk.

The density of the samples was measured by the buoyancy method using polished plates prior to cutting (Kern&Sohn, Lörrach, Germany). Vickers hardness measurements HV10 (n = 5) (Bareiss, Oberdischingen, Germany) were carried out to determine the hardness and the indentation fracture toughness K_{DCM} by direct crack length measurements. The indentation toughness was calculated according to the Niihara Palmqvist crack model [25]. For the fully dense Y-TZP samples, a Young's modulus of 210 GPa was assumed [15]. Four-point bending tests were carried out in a setup with 20 mm outer and 10 mm inner span at a crosshead speed of 0.5 mm/min (n = 12) (ZwickRoell, Ulm, Germany). Indentation strength in bending (ISB) tests were carried out in the same setup at 2.5 mm/min crosshead speed. For the ISB tests, the samples were indented with 4 indents at a distance of 2 mm with cracks parallel and perpendicular to the sides. The indented region was placed on the tensile side within the inner span and the residual strength was measured. Placing dummy indentations was necessary due to the inhomogeneity of the crack patterns in order to obtain at least one valid indentation per bar. The ISB toughness K_{ISB} was then calculated using the model of Chantikul [26]. It is known from literature that in understabilized Y-TZP materials transformation zones around the indents may cause crack trapping effects, which lead to overestimated toughness values [27]. Hence, a modified SIGB (stable indentation crack growth in bending) test according to Dransmann was applied [28]. In order to suppress transformation and obtain starter cracks exceeding

the transformation zone around the crack, HV10 Vickers indents were introduced at elevated temperature (250–300 °C). The samples were then progressively loaded at 5 mm/min and the crack growth was measured after each loading step (n = 2 with 4 indents each). A detailed description of the SIGB test is given by Benzaid [29].

The phase composition of as-fired samples without preparation and polished samples in the 27–33° 2θ range (containing the −111, 111 monoclinic and the 101 tetragonal peaks) was measured by XRD (X'Pert MPD, Panalytical, Eindhoven, The Netherlands, CuKα1, Ge-monochromator, Bragg-Brentano setup, accelerator detector) according to the protocol of Toraya [30]. The phase composition was also determined in fracture surfaces in order to determine the transformability and the transformation zone size according to Kosmac [31]. The fourth order peaks in the 72–75° 2θ range were studied to obtain tetragonality values and confirm absence of cubic phase. The crystallite size in the starting powder was estimated using the Scherrer analysis tool of Highscore (Panalytical, Eindhoven, The Netherlands) software package.

The transformation toughness values were calculated according to McMeeking and Evans assuming a transformation efficiency of 0.27 (predominantly dilational transformation) [32].

SEM images were taken from polished and thermally etched samples (10 °C/min to 1150 °C, 10 dwell in air) in order to determine the grain size [33] and identify possible thermal transformation effects. SEM was also used to characterize the powder and granulate.

The tensile sides of fractured bars were checked by optical microscopy for formation of transformation bands which would indicate transformation related failure [34].

3. Results

3.1. Powder Characterization

Figure 1a shows an SEM image of spray dried granules of the RTP granulate. Granules are perfectly round; they have a smooth surface and are free of defects and satellites. The size of the individual granules varies between 15 and 50 µm; the average size correlates to manufacturer's specification. Figure 1b shows an image of the granulate surface with size markers for different grains. The grains are compact and densely packed, with a size range of 40–140 nm. Only a few agglomerates are visible. XRD analysis shows that the phase composition of the starting powder is 94 vol% monoclinic and 6% tetragonal. The average crystallite size estimated from the line broadening of the monoclinic −111 and 111 peaks is 40 ± 2.5 nm. The block-shaped structure of the grains and the predominantly monoclinic phase composition implies that the powder has been milled to size.

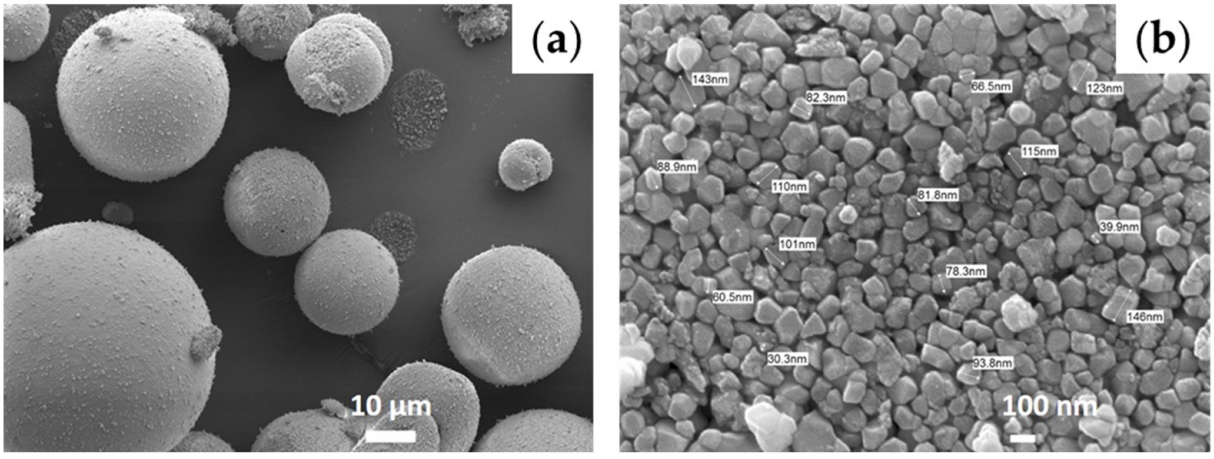

Figure 1. SEM images of ready-to-press (RTP) granulate: (**a**) granules, (**b**) grains embedded in granulate.

3.2. Density and Mechanical Properties

The density ρ/ρ_{th} of the TZP samples sintered at different temperatures is shown in Figure 2. Evidently, sintering at 1250 °C is not sufficient to obtain fully dense material (relative density 97.9%). At sintering temperatures ≥ 1300 °C, the obtained materials are practically fully dense (99.3–99.7% assuming a theoretical density of ρ_{th} = 6.1 g/cm^3).

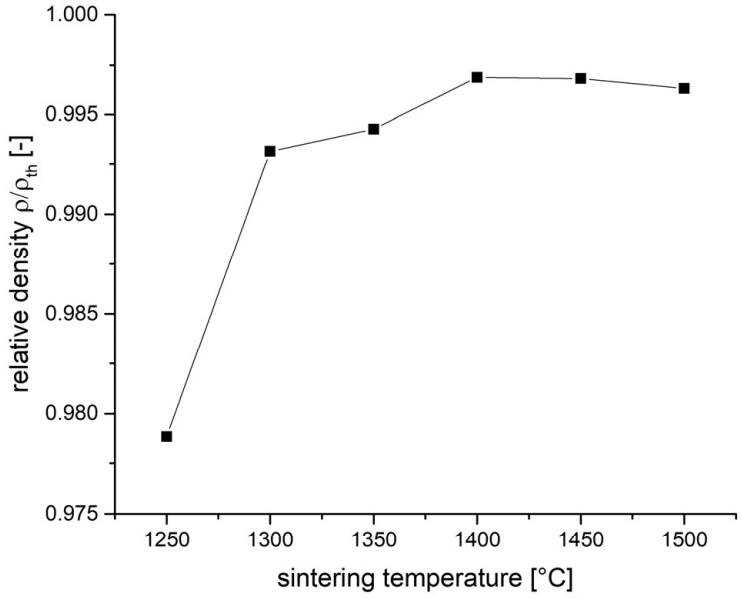

Figure 2. Relative density ρ/ρ_{th} of TZP samples sintered at different temperatures.

Figure 3 shows the Vickers hardness HV10 and the bending strength σ_{4pt} of the TZPs sintered at different temperatures. The Vickers hardness shows a strong correlation to the density values. The hardness increases from 1175 HV10 to 1250 HV10 between 1250 and 1300 °C. Then, the hardness further increases until 1400 °C. The slight reduction in hardness at even higher temperatures is probably related to increasing grain size. All samples reach average bending strength values >1200 MPa. The strength maximum is obtained at 1350 °C with 1440 ± 110 MPa. Direct evidence for transformation-induced failure, such as transformation bands on the tensile side of fractured bars or non-linearity of stress–strain curves, were not observed.

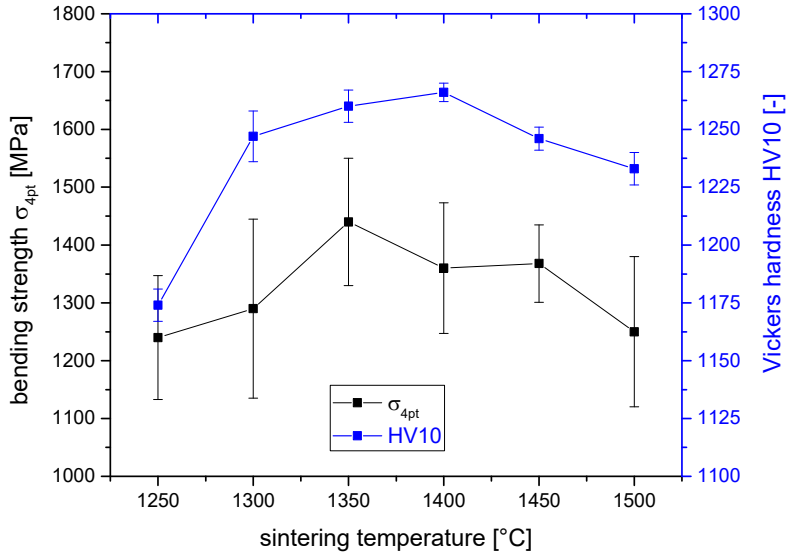

Figure 3. Vickers hardness HV10 and bending strength σ_{4pt} of TZPs sintered at different temperatures.

Figure 4 compares the toughness values determined by direct crack length measurement K_{DCM} and by indentation strength in bending K_{ISB}. In both cases, samples were indented at ambient temperature. Note: Both calculation methods require a value for the Young's modulus E; E was assumed as 210 GPa for all samples except the sample sintered at 1250 °C which was not dense (assumed value 200 GPa).

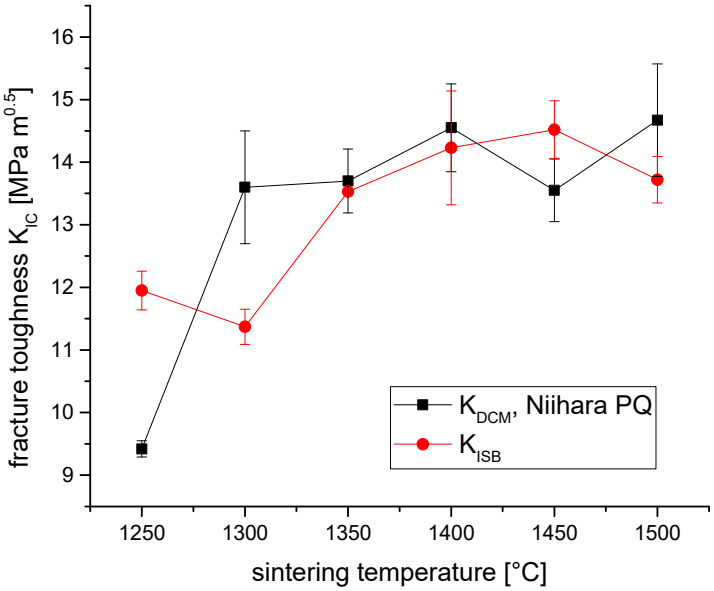

Figure 4. Fracture toughness values K_{DCM} and K_{ISB} of TZPs sintered at different temperatures.

The toughness levels determined by both testing protocols are comparable and extremely high. Maximum values of 13–15 MPa$\sqrt{m}$ were measured at sintering temperatures between 1300 °C and 1500 °C. These results correlate very well with indentation toughness data obtained by Billovits for the same material [35] and Matsui for ZGAIA 1.5Y-TZP [16]. Realistically, the strength–toughness correlations published by Swain [36] raise some doubts about the correctness of these indentation-based toughness values. With the given strength of 1200–1440 MPa (strength can be measured reliably), the corresponding toughness can be achieved either on the defect size-related branch of the curve at 6 MPa$\sqrt{m}$ or on the transformation-dominated side at 8 MPa$\sqrt{m}$ (note that Swain's data are indentation toughness data; strength data are from 3pt measurements). Moreover, the observed crack patterns which are frequently incomplete are a clear indication of trapping effects. As the ISB test is based on the assumption of semicircular crack geometries (geometry factor Y = 1.27), a correction factor needs to be introduced. Dransmann experimentally determined a value of Y = 1.08 for 3Y-TZP [28]. In the present case of even tougher 2Y-TZP, we assumed Y = 0.95. This would reduce the uncorrected maximum ISB-toughness values by 25% to corrected values of ~10.5 MPa$\sqrt{m}$.

The following graph (Figure 5) shows the fracture toughness values determined from the strongest survivors in the SIGB test using samples which were indented at elevated temperature. Note that no extrapolation to infinite crack lengths was carried out which may lead to a slight underestimation of toughness [28,29]. The sample sintered at 1500 °C was not measurable. It was thermally instable and transformed during the heating procedure. For the peak toughness materials, indentation at 250 °C increases the crack length 2c (from crack tip to crack tip in a HV10 indent) from approximately 0.14 µm to 0.18 µm. In fact, as expected due to larger starting cracks and suppression of transformation-induced crack trapping, the warm-indented samples fail at stress levels of 500–540 MPa. ISB samples indented at ambient temperature reach residual strength levels of 1000 MPa. The toughness levels by SIGB range from 5.5 MPa$\sqrt{m}$ to 7.8 MPa$\sqrt{m}$. Such values seem reasonable with respect to Swains reference data [36]. The maximum toughness is achieved at 1350 °C sintering temperature. The toughness dip at 1300 °C is probably related to the incomplete

densification at 1250 °C. The presence of porosity in the 1250 °C sample reduces the elastic constraint and facilitates transformation. Moreover, pores may stop cracks. The same toughness minimum at 1300 °C is seen in ISB-toughness values (Figure 4).

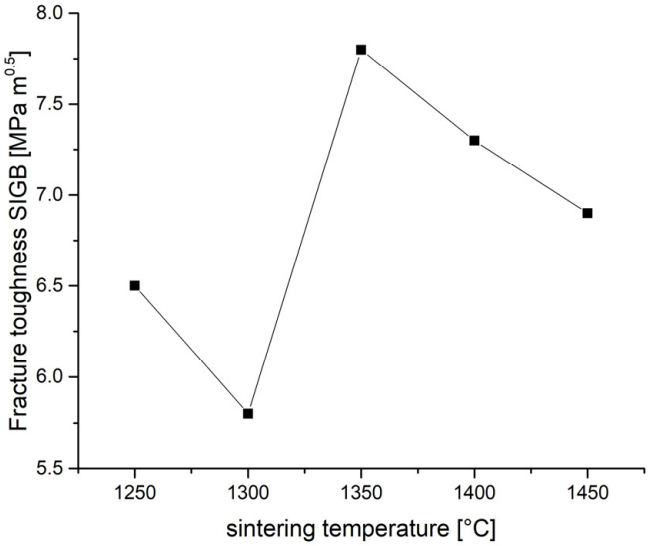

Figure 5. Fracture toughness values K_{SIGB} of TZPs sintered at different temperatures; samples notched at elevated temperature.

3.3. Microstructure

Figure 6 shows the microstructure of polished and thermally etched samples sintered at different sintering temperatures. Considerable porosity is visible in the sample sintered at 1250 °C/2 h. At higher sintering temperatures porosity is significantly reduced. Some isolated pores are visible even at the highest sintering temperature. Microstructure images are in accord with measured densities (Figure 2).

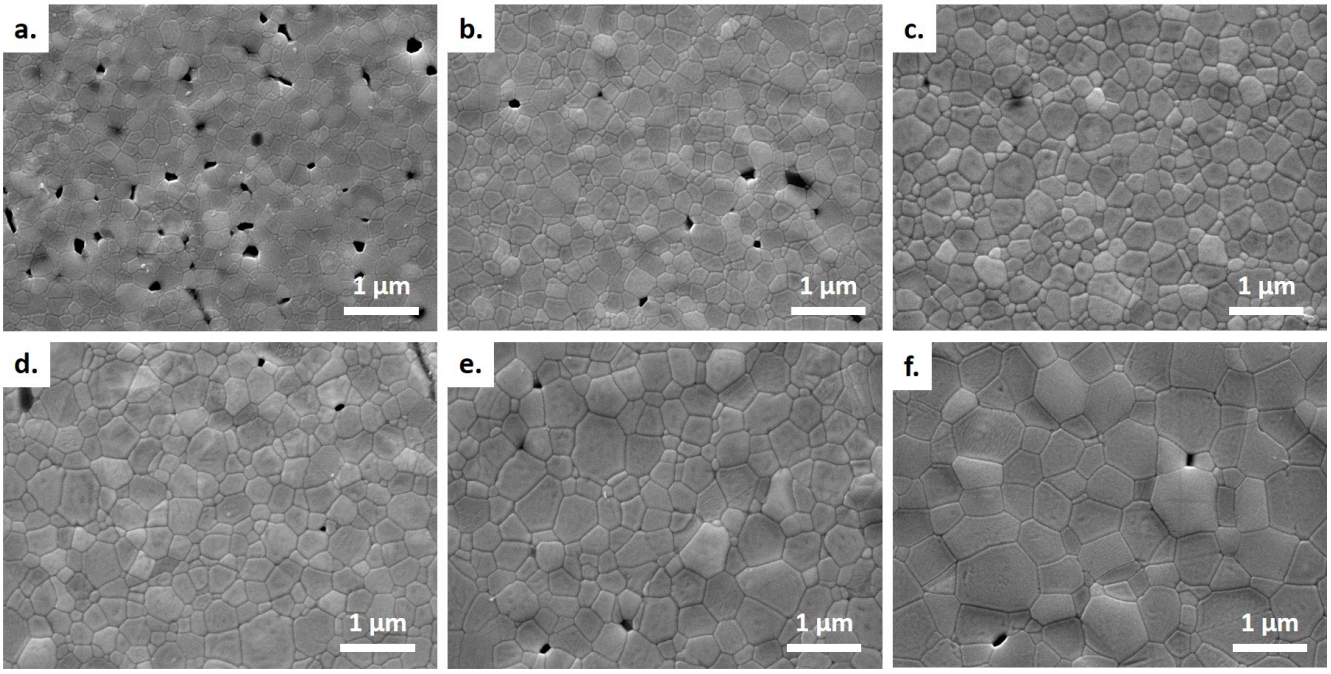

Figure 6. Microstructure of 2Y-TZP (polished and thermally etched surfaces). (**a**) 1250 °C/2 h; (**b**) 1300 °C/2 h; (**c**) 1350 °C/2 h; (**d**) 1400 °C/2 h; (**e**) 1450 °C/2 h; (**f**) 1500 °C/2 h.

The uneven surface structure especially at sintering temperatures > 1400 °C may indicate a certain degree of t-m phase transformation after thermal etching associated with volume expansion. Figure 7 shows the evolution of average grain size with sintering temperature. As expected, the grain size increases with sintering temperature. Considering a maximum grain size of 400 nm as required for high-strength dental applications (three or more element bridges) according to EN 6872, the sintering temperature should be limited to 1350–1400 °C.

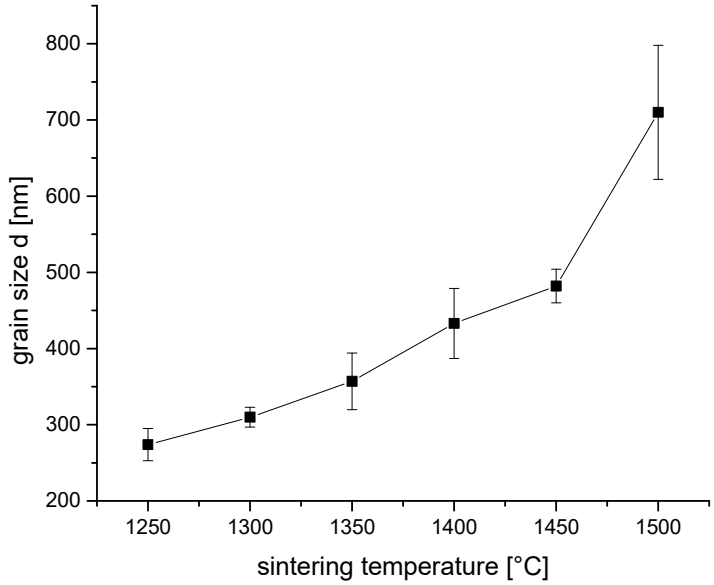

Figure 7. Grain size of 2Y-TZP determined by line intercept method (correction factor 1.56).

3.4. Phase Composition and Transformation Toughening Effect

Figure 8 shows the XRD traces of as-fired surfaces (a) and fracture surfaces (b) of 2Y-TZP sintered at different temperatures in the monoclinic/tetragonal fingerprint range between 27 and 33° 2θ. In case of polished TZP surfaces, the intensity of the monoclinic peaks is almost negligible, see Figure 8a. Besides the dominant 101_t peak at 30.2° 2θ, only the -111_m peak at 28.1° 2θ is clearly distinguishable. In Figure 8b, all three peaks can be clearly seen. A decline of the intensity of the 101 peak of tetragonal phase and a concurrent increase of the intensity of the −111 and 111 peaks of monoclinic phase with increasing sintering temperature are clearly visible. Hence, the transformability of tetragonal phase increases with sintering temperature.

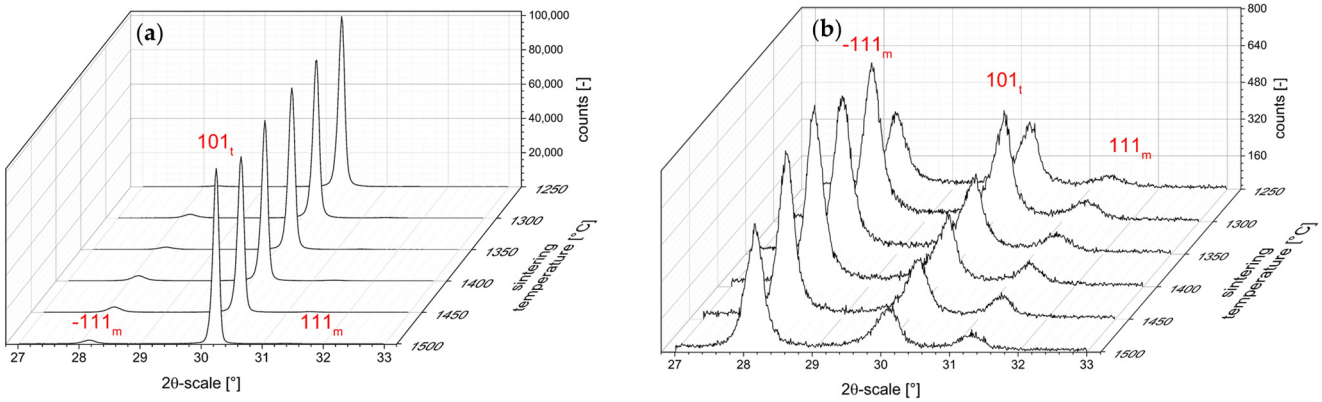

Figure 8. XRD traces in the t-m fingerprint range of 2Y-TZP sintered at different temperatures: (**a**) as-fired surfaces; (**b**) fracture surfaces.

Figure 9 summarizes the quantitative evaluation of the XRD studies and shows the monoclinic contents in as-fired surfaces, polished surfaces and fracture surfaces of bars after 4pt bending test. The as-fired surfaces exhibit a considerable monoclinic content which increases from 3 vol.% at 1250 °C to 13 vol.% at 1450 °C sintering temperature. The polished surfaces show significantly lower monoclinic contents in the range of 1–2 vol.%. Seemingly, the as-fired surface suffers from transformation during cooling, while the bulk is almost entirely tetragonal. The monoclinic content in the fracture surfaces increases with sintering temperature from 61 vol.% at 1250 °C to 75 vol.% at 1400 °C, then no further increase is observed. At high sintering temperature, the measured monoclinic contents are close to the theoretically possible values of ~85 vol.% quoted by Mamivand [37]. The transformability V_f, which is required to calculate the transformation toughness, is calculated as $V_f = V_{m,FF} - V_{m,pol}$.

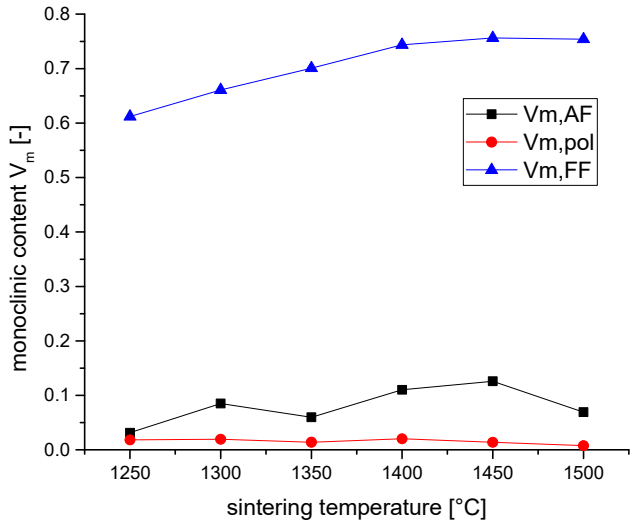

Figure 9. Monoclinic contents of TZP materials sintered at different temperatures measured by XRD $V_{m,AF}$ in as-fired surface, $V_{m,pol}$ in polished surface and $V_{m,FF}$ in fracture surface.

Figure 10 shows the transformation zone sizes h according to Kosmac [31] and the corresponding transformation toughness values $\Delta K_{IC}{}^{T}$ according to McMeeking [32], which were obtained by evaluation of XRD data of polished and fractured surfaces.

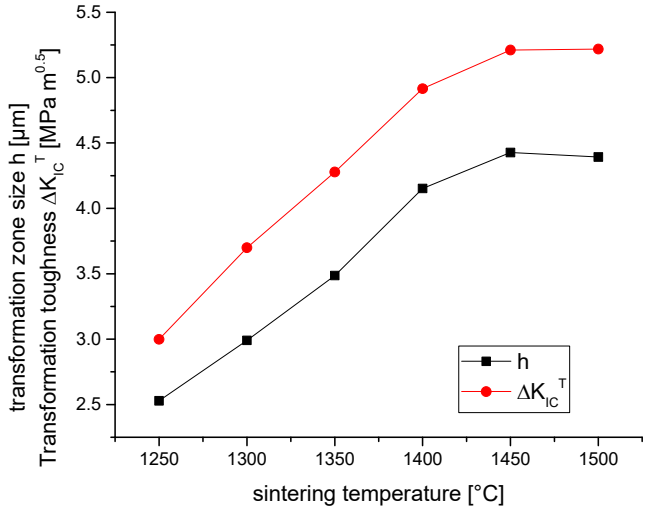

Figure 10. Transformation zone size h and transformation toughness $\Delta K_{IC}{}^{T}$ of TZP materials sintered at different temperatures.

Transformation zone sizes reach a maximum of 4.5 µm at sintering temperatures between 1400 and 1500 °C. The calculated transformation toughness increases from 3 MPa$\sqrt{m}$ at 1250 °C to 5 MPa$\sqrt{m}$ at 1400 °C. At 1450–1500 °C TT levels off.

Assuming that toughening effects are additive, the total fracture toughness can be calculated as $K_{IC} = K_0 + K_{IC}{}^T$ in absence of other toughening mechanisms than TT. Literature data for the crack tip toughness or intrinsic toughness K_0 (in absence of reinforcement effects) are between K_0 = 3 MPa$\sqrt{m}$ [29] and K_0 = 4 MPa$\sqrt{m}$ [36,38]. Therefore, on the basis of XRD data and theoretical considerations, the maximum toughness of the material may not exceed 8–9 MPa$\sqrt{m}$. This implies that both DCM and ISB values (Figure 4) are exaggerated and that the measured SIGB toughness data (Figure 5) are within the calculated range or slightly below.

4. Discussion

The 2Y-TZP material investigated shows an attractive combination of strength and fracture toughness. An in-depth study of transformation behavior and calculation of the maximum transformation toughness increment confirms that direct crack length measurement and ISB tests both lead to drastic overestimations of the fracture toughness values. The reason for this can be found in crack-trapping effects as described by Cook [27]. The cracks induced by HV10 indents are trapped in the transformation zone resulting not only in extremely short crack lengths but also very frequently in irregular crack patterns which are difficult to interpret. Similar conclusions are obtained comparing the results of Matsui and Imariouane who studied a quite similar understabilized 1.5Y-TZP material [16,17]. In ISB tests, cracks are extended due to tensile stress during loading the sample to failure. However, if the cracks are trapped within the transformation zone, the sample will fail at short crack extension immediately when the crack exits the shielded zone around the indent rather than grow evenly. This sudden bursting of ISB bars resulted in residual strength levels of up to 1000 MPa. The chosen procedure to place indentations at elevated temperature (250–300 °C) at least reduces the transformability and allows the cracks to grow during the SIGB test. However, this solution cannot be applied in all samples, the sample sintered at 1500 °C turned out to be vulnerable to heating and transformed; hence, no measurement of the sample sintered at this temperature was possible (Figure 5). XRD measurements and the calculation of fracture toughness using the model of McMeeking and Evans [32] allows to estimate the possible maximum toughness in this 2Y-TZP (8–9 MPa$\sqrt{m}$). The SIGB tests carried out with samples indented at elevated temperature lead to toughness values within or below this range. It has to be considered that samples are small, and toughness values were not extrapolated to larger crack lengths; this may account for slight underestimations. Moreover, a constant transformation efficiency of X = 0.27 (predominantly but not exclusively dilational) was applied for calculation. It could be that at high sintering temperatures and large grain sizes the transformation efficiency may decline as in the case of Ce-TZP materials [2].

Another point worth discussing in the context of Ref. [18] is the elevated monoclinic content of the as-fired surface compared to polished surfaces. Thermal etching also leads to uneven surfaces especially for samples sintered at higher temperatures. In the sintering cycles for the study, the samples were cooled down with 12 °C/min (or in the case of lower temperature, as fast as the thermal inertia of the furnace allowed it). These observations of thermal vulnerability are in line with results of Imariouane on ageing of 1.5Y-TZP [18]. Maybe even faster cooling would be beneficial to prevent phase transformation. This increases the requirements of the furnace and kiln furniture and indicates possible difficulties in net-shape manufacturing of larger components.

The starting powder is relatively coarse and homogeneous in grain size but, nevertheless, very sinterable. This is a favorable combination in terms of processability, not only by pressing but also by other shaping technologies such as ceramic injection molding or stereolithography.

A comparison with literature values (Table 1) shows that the tested pressureless sintered 2Y-TZP shows a similar toughness as other 1.5-2Y TZP materials that were tested using conservative methods. The strength is slightly higher than recently determined for 1.5Y-TZP [17], which is probably due to the absence of transformation-induced failure.

5. Conclusions

The alumina-doped 2Y-TZP tested in this study provides a combination of high toughness and high strength, which makes the material attractive for structural applications requiring high damage tolerance for catastrophic events. Transformation toughness increments of up to 5 MPa$\sqrt{m}$ represent the maximum of the theoretically possible value for Y-TZP materials. Transformation-induced failure was not observed. However, as the R-curve dependent toughness is so high the materials are probably prone to suffer from sub-critical crack growth, i.e., they are not well suited to bear high constant or alternating loads. Indentation-based measurements may lead to overestimation of fracture toughness due to crack trapping and result in mistakes in the design of components. The best sintering condition is probably 1350 °C/2h. Here, both strength and toughness reach their optimum, grain growth is still moderate and the material is fully dense. Overfiring shifts the material into the transformation-dominated range. Strength and toughness decrease and low temperature degradation may become an issue.

Author Contributions: Conceptualization, F.K.; investigation F.K. and B.O.; writing—original draft preparation, F.K.; writing—review and editing, F.K. and B.O.; visualization, B.O. All authors have read and agreed to the published version of the manuscript.

Funding: This research received no external funding.

Institutional Review Board Statement: Not applicable.

Informed Consent Statement: Not applicable.

Data Availability Statement: The raw data supporting the conclusions of this article will be made available by the authors on request.

Conflicts of Interest: The authors declare no conflicts of interest.

References

1. Hannink, R.H.J.; Kelly, P.M.; Muddle, B.C. Transformation Toughening in Zirconia-Containing Ceramics. *J. Am. Ceram. Soc.* **2000**, *83*, 461–487. [CrossRef]
2. Kelly, P.M.; Rose, L.R.F. The martensitic transformation in ceramics—Its role in transformation toughening. *Prog. Mater. Sci.* **2002**, *47*, 463–557. [CrossRef]
3. Rose, L.R.F. The mechanics of transformation toughening. *Proc. R. Soc. Lond. A* **1987**, *412*, 169–197. [CrossRef]
4. Li, P.; Chen, I.-W.; Penner-Hahn, J.E. Effect of Dopants on Zirconia Stabilization—An X-ray Absorption Study: I, Trivalent Dopants. *J. Am. Ceram. Soc.* **1994**, *77*, 118–128. [CrossRef]
5. Li, P.; Chen, I.-W.; Penner-Hahn, J.E. Effect of Dopants on Zirconia Stabilization—An X-ray Absorption Study: II, Tetravalent Dopants. *J. Am. Ceram. Soc.* **1994**, *77*, 1281–1288. [CrossRef]
6. Chen, M.; Hallstedt, B.; Gauckler, L.J. Thermodynamic modeling of the ZrO_2–$YO_{1.5}$ system. *Solid State Ion.* **2004**, *170*, 255–274. [CrossRef]
7. Kelly, J.R.; Denry, I. Stabilized zirconia as a structural ceramic: An overview. *Dent. Mater.* **2008**, *24*, 289–298. [CrossRef]
8. Matsui, K.; Yoshida, H.; Ikuhara, Y. Phase-transformation and grain-growth kinetics in yttria-stabilized tetragonal zirconia polycrystal doped with a small amount of alumina. *J. Eur. Ceram. Soc.* **2010**, *30*, 1679–1690. [CrossRef]
9. Chevalier, J.; Gremillard, L.; Virkar, A.V.; Clarke, D.R. The Tetragonal-Monoclinic Transformation in Zirconia: Lessons Learned and Future Trends. *J. Am. Ceram. Soc.* **2009**, *92*, 1901–1920. [CrossRef]
10. Ruiz, L.; Readey, M.J. Effect of Heat Treatment on Grain Size, Phase Assemblage, and Mechanical Properties of 3 mol% Y-TZP. *J. Am. Ceram. Soc.* **1996**, *79*, 2331–2340. [CrossRef]
11. Binner, J.; Vaidhyanathan, B.; Paul, A.; Annaporani, K.; Raghupathy, B. Compositional Effects in Nanostructured Yttria Partially Stabilized Zirconia. *Int. J. Appl. Ceram. Technol.* **2011**, *8*, 766–782. [CrossRef]
12. Chevalier, J.; Cales, B.; Drouin, M. Low-Temperature Aging of Y-TZP Ceramics. *J. Am. Ceram. Soc.* **1999**, *82*, 2150–2154. [CrossRef]
13. Lange, F.F. Transformation toughening: Part 3 Experimental observations in the ZrO_2- Y_20_3 system. *J. Mater. Sci.* **1982**, *17*, 240–246. [CrossRef]

14. Tsukuma, K. Thermal and Mechanical Properties of Y_2O_3-Stabilized Tetragonal Zirconia Polycrystals, Science and Technology of Zirconia II. *Adv. Ceram.* **1984**, *12*, 382–390.
15. Kern, F.; Reveron, H.; Chevalier, J.; Gadow, R. Mechanical behaviour of extremely tough TZP bioceramics. *J. Mech. Behav. Biomed. Mater.* **2019**, *90*, 395–403. [CrossRef] [PubMed]
16. Matsui, K.; Hosoi, K.; Feng, B.; Yoshida, H.; Ikuhara, Y. Ultrahigh toughness zirconia ceramics. *Proc. Natl. Acad. Sci. USA* **2023**, *120*, e2304498120. [CrossRef] [PubMed]
17. Imariouane, M.; Saâdaoui, M.; Denis, G.; Reveron, H.; Chevalier, J. Low-yttria doped zirconia: Bridging the gap between strong and tough ceramics. *J. Eur. Ceram. Soc.* **2023**, *43*, 4906–4915. [CrossRef]
18. Imariouane, M.; Saâdaoui, M.; Cardinal, S.; Reveron, H.; Chevalier, J. Aging behavior of a 1.5 mol% yttria doped zirconia exhibiting optimized toughness and strength. *J. Eur. Ceram. Soc.* **2024**, *44*, 1053–1060. [CrossRef]
19. Kern, F. *Neue Oxidkeramiken und Nanocomposites für Hochleistungsanwendungen*; Shaker Verlag: Aachen, Germany, 2016; ISBN 3844049010.
20. Akhlaghi, O.; Camposilvan, E.; Goharibajestani, Z.; Abkenar, S.K.; Ow-Yang, C.W.; Jorand, Y.; Gremillard, L.; Garnier, V.; Chevalier, J. Transparent high-strength nanosized yttria stabilized zirconia obtained by pressure-less sintering. *J. Eur. Ceram. Soc.* **2022**, *42*, 7187–7195. [CrossRef]
21. Roitero, E.; Reveron, H.; Gremillard, L.; Garnier, V.; Ritzberger, C.; Chevalier, J. Ultra-fine Yttria-Stabilized Zirconia for dental applications: A step forward in the quest towards strong, translucent and aging resistant dental restorations. *J. Eur. Ceram. Soc.* **2023**, *43*, 2852–2863. [CrossRef]
22. Cui, J.; Gong, Z.; Lv, M.; Rao, P. Determination of fracture toughness of Y-TZP ceramics. *Ceram. Int.* **2017**, *43*, 16319–16322. [CrossRef]
23. Basu, B.; Vleugels, J.; van der Biest, O. Toughness tailoring of yttria-doped zirconia ceramics. *Mater. Sci. Eng. A* **2004**, *380*, 215–221. [CrossRef]
24. Trunec, M.; Stastny, P.; Kastyl, J.; Roupcova, P.; Chlup, Z. 2Y-TZP ceramics with high strength and toughness by optimizing the microstructure. *J. Eur. Ceram. Society* **2024**, *44*, 3258–3266. [CrossRef]
25. Niihara, K. A fracture mechanics analysis of indentation-induced Palmqvist crack in ceramics. *J. Mater. Sci. Lett.* **1983**, *2*, 221–223. [CrossRef]
26. Chantikul, P.; Anstis, G.R.; Lawn, B.R.; Marshall, D.B. A Critical Evaluation of Indentation Techniques for Measuring Fracture Toughness: II, Strength Method. *J. Am. Ceram. Soc.* **1981**, *64*, 539–543. [CrossRef]
27. Cook, R.F.; Braun, L.M.; Cannon, W.R. Trapped cracks at indentations: Part I: Experiments on yttria-tetragonal zirconia polycrystals. *J. Mater. Sci.* **1994**, *29*, 2133–2142. [CrossRef]
28. Dransmann, G.W.; Steinbrech, R.W.; Pajares, A.; Guiberteau, F.; Dominguez-Rodriguez, A.; Heuer, A.H. Indentation Studies on Y_2O_3-Stabilized ZrO_2: II, Toughness Determination from Stable Growth of Indentation-Induced Cracks. *J. Am. Ceram. Soc.* **1994**, *77*, 1194–1201. [CrossRef]
29. Benzaid, R.; Chevalier, J.; Saadaoui, M.; Fantozzi, G.; Nawa, M.; Diaz, L.A.; Torrecillas, R. Fracture toughness, strength and slow crack growth in a ceria stabilized zirconia-alumina nanocomposite for medical applications. *Biomaterials* **2008**, *29*, 3636–3641. [CrossRef]
30. Toraya, H.; Yoshimura, M.; Somiya, S. Calibration Curve for Quantitative Analysis of the Monoclinic-Tetragonal ZrO_2 System by X-Ray Diffraction. *J. Am. Ceram. Soc.* **1984**, *67*, C119–C121. [CrossRef]
31. Kosmać, T.; Wagner, R.; Claussen, N. X-Ray Determination of Transformation Depths in Ceramics Containing Tetragonal ZrO_2. *J. Am. Ceram. Soc.* **1981**, *64*, C-72–C-73. [CrossRef]
32. McMeeking, R.M.; Evans, A.G. Mechanics of Transformation-Toughening in Brittle Materials. *J. Am. Ceram. Soc.* **1982**, *65*, 242–246. [CrossRef]
33. Mendelson, M.I. Average Grain Size in Polycrystalline Ceramics. *J. Am. Ceram. Soc.* **1969**, *52*, 443–446. [CrossRef]
34. Liens, A.; Swain, M.; Reveron, H.; Cavoret, J.; Sainsot, P.; Courtois, N.; Fabrègue, D.; Chevalier, J. Development of transformation bands in ceria-stabilized-zirconia based composites during bending at room temperature. *J. Eur. Ceram. Soc.* **2021**, *41*, 691–705. [CrossRef]
35. Billovits, T.; Demel-Eckhart, S. Exploring the Boundaries of Strength and Toughness: AuerTec® 2Y-40A, Extended Abstract ECERS XVIII, Lyon, France. Available online: https://www.ecers2023.org/data/onglet34/module0/modalPreview.php?langue=fr&paramProjet=89 (accessed on 15 May 2024).
36. Swain, M.V.; Rose, L.R.F. Strength Limitations of Transformation-Toughened Zirconia Alloys. *J. Am. Ceram. Society* **1986**, *69*, 511–518. [CrossRef]

37. Mamivand, M.; Asle Zaeem, M.; El Kadiri, H. Phase field modeling of stress-induced tetragonal-to-monoclinic transformation in zirconia and its effect on transformation toughening. *Acta Mater.* **2014**, *64*, 208–219. [CrossRef]
38. Evans, A.G. Perspective on the Development of High-Toughness Ceramics. *J. Am. Ceram. Soc.* **1990**, *73*, 187–206. [CrossRef]

Disclaimer/Publisher's Note: The statements, opinions and data contained in all publications are solely those of the individual author(s) and contributor(s) and not of MDPI and/or the editor(s). MDPI and/or the editor(s) disclaim responsibility for any injury to people or property resulting from any ideas, methods, instructions or products referred to in the content.